

Migration and the formation of systems of hot super-Earths and Neptunes

Caroline Terquem^{1,2}

Institut d'Astrophysique de Paris, UMR7095 CNRS, Université Pierre & Marie Curie-Paris 6, 98bis boulevard Arago, 75014 Paris, France

terquem@iap.fr

and

John C. B. Papaloizou

Department of Applied Mathematics and Theoretical Physics, University of Cambridge, Centre for Mathematical Sciences, Wilberforce Road, Cambridge, CB3 0WA, UK

J.C.B.Papaloizou@damtp.cam.ac.uk

ABSTRACT

The existence of extrasolar planets with short orbital periods suggests that planetary migration induced by tidal interaction with the protoplanetary disk is important. Cores and terrestrial planets may undergo migration as they form. In this paper we investigate the evolution of a population of cores with initial masses in the range 0.1–1 earth mass embedded in a disk. Mutual interactions lead to orbit crossing and mergers, so that the cores grow during their evolution. Interaction with the disk leads to orbital migration, which results in the cores capturing each other in mean motion resonances. As the cores migrate inside the disk inner edge, scatterings and mergers of planets on unstable orbits together with orbital circularization causes strict commensurability to be lost. Near commensurability however is usually maintained. All the simulations end with a population of typically between two and five planets, with masses depending on the initial mass. These results indicate that if hot super-Earths or Neptunes form by mergers of inwardly migrating cores, then such planets are most likely not isolated. We would expect to always find at least one, more likely a few,

¹Université Denis Diderot-Paris 7, 2 Place Jussieu, 75251 Paris Cedex 5, France

²Institut Universitaire de France

companions on close and often near-commensurable orbits. To test this hypothesis, it would be of interest to look for planets of a few to about 10 earth masses in systems where hot super-Earths or Neptunes have already been found.

Subject headings: planetary systems: formation — planetary systems: protoplanetary disks

1. Introduction

The recent announcements of the detection of extrasolar planets of a few earth masses (M_{\oplus}) (OGLE-05-390L b, $5.4 M_{\oplus}$, Beaulieu et al. 2006; Gliese 876 d, $7.3 M_{\oplus}$, Rivera et al. 2005) gives support to the initial solid core accumulation model for planet formation. Although it has been proposed that such “super-Earths” could have formed through gravitational instability in a gaseous protoplanetary disk leading to a giant planet which subsequently lost its gaseous envelope through the action of external UV radiation (Boss 2006), a formation mechanism through the accumulation of planetesimals seems more natural. In addition to these super-Earths, nine planets with a mass comparable to that of Uranus or Neptune (in the range 10.5 to $18.5 M_{\oplus}$) have been reported.

OGLE-05-390L b is at a distance of 2.1 astronomical unit (au) from the central star and was detected through microlensing. Gliese 876 d, detected through radial velocity measurements, is at 0.02 au from its parent star. Among the nine planets with masses similar to that of Neptune, four are within 0.1 au from the central star.

Gliese 876 is a M-type star. The temperature at 0.02 au from the star is therefore low enough for heavy elements to condense. Thus it is possible to consider that Gliese 876 d formed *in situ* by accumulation of heavy material that spiraled in with the gas through the circumstellar disk. However, the existence of close orbiting giant planets, the so-called ‘hot Jupiters’ and ‘hot Neptunes’, has been taken as an indication of the operation of large scale migration induced by the interaction of recently formed protoplanets with protoplanetary disks (e.g., Papaloizou & Terquem 2006 and references therein). Such migration processes may have operated during the formation of lower mass planets as well. In particular, planets in the earth mass range are expected to undergo type I migration (e.g., Ward 1997). Accordingly, here we envisage a scenario in which cores assemble further away from the central star, and migrate inwards due to tidal interaction with the disk. The disk is supposed to be truncated at some inner edge so that the planets do not fall onto the star. Mutual perturbations of the cores leads to orbit crossing, collisions and possibly mergers during the migration phase, resulting in the formation of a smaller number of more massive planets on

short period orbits.

Such a scenario has been considered by Brunini & Cionco (2005), who calculated by means of N -body simulations the evolution of 100 protoplanets of $0.5 M_{\oplus}$ together with 200 planetesimals of $0.1 M_{\oplus}$ subject to their mutual interaction and the tidal interaction with the disk. Focusing on the mass and semi-major axis of the final largest solid core, they concluded that Neptune-like planets on short orbits should be common.

Here we focus on the final configuration of the multi-planet systems we obtain. Evolution of an ensemble of cores in a disk almost always leads to a system of a few planets, with masses that depend on the total initial mass, on short orbits with mean motions that frequently exhibit near commensurabilities and, for long enough tidal circularization times, apsidal lines that are locked together. Starting with a population of 10 to 25 planets of 0.1 or $1 M_{\oplus}$, we end up with typically between two and five planets with masses of a few tenths of an earth mass or a few earth masses, depending on the total initial mass, inside the disk inner edge. Interaction with the central star leads to tidal circularization of the orbits which, together with possible close scatterings and final mergers, tends to disrupt mean-motion resonances that are established during the migration phase. The system, however, often remains in a configuration in which the orbital periods are close to commensurability. Apsidal locking of the orbits, if established during migration, is often maintained through the action of these processes.

The plan of the paper is as follows. In section 2, we review studies of the evolution of migrating resonant planets. We also show that tidal circularization by the central star results in the disruption of strict commensurability, although the mean motions may remain nearly commensurable and apsidal lines remain locked. In section 3, we describe the model we use to follow the evolution of a population of planets, and describe our initial conditions. To calculate the mutual interactions between the cores, we use a N -body code. A dissipative force is included to model the tidal interaction with the disk, which leads to orbital decay and eccentricity and inclination damping. Relativistic effects and tidal interaction with the central star are also included, as they affect the eccentricity of the orbits close to the star. We also incorporate the possibility of corotation torques acting in the edge region. The potential importance of these in reversing type I migration has been indicated by Masset et al. (2006). We discuss the effects of such torques on eccentric orbits. In section 4, we describe our results. As mentioned above, all the runs end with a few planets on close orbits inside the inner cavity that frequently exhibit near commensurability and apsidal line locking. We study the effect of varying the circularization timescale and of a hypothetical reversal of the torque near the disk inner edge due to corotation or other effects. Finally, in section 5, we summarize and discuss our results.

2. Migration of planets and orbital resonance

2.1. Resonant capture during migration

The existence of commensurabilities among the mean motions of pairs of satellites of Jupiter and Saturn is believed to be the result of capture into resonances following the differential expansion of their orbits induced by the dissipation of the tides raised in the central planet (Greenberg et al. 1972, Greenberg 1973). Once established, such commensurabilities are stable due to the secular transfer between the satellites of the angular momentum fed into the satellite system by the tides (Goldreich 1965). Planets in a disk may also get locked into a resonance if their semi-major axes evolve at a different rate causing their orbits to approach each other. Melita & Woolfson (1996; see also Haghighipour 1999) were first to consider such a scenario to explain near-commensurability between the periods of the major planets of the solar system. In their study, the evolution of the semi-major axes was assumed to be caused by accretion of gas by the planets and dynamical friction. Kley (2000) subsequently studied the evolution of two Jupiter-like planets embedded in a protoplanetary disk that underwent orbital migration due to tidal interaction with the disk. Formation and maintenance of commensurabilities in a system of migrating planets in this type of simulation was subsequently reported by Masset & Snellgrove (2001) and Snellgrove et al. (2001). Since then, different studies, motivated by the observation of extrasolar planetary systems exhibiting commensurabilities, have shown that capture of giant planets into resonances during migration is a natural expectation (Nelson & Papaloizou 2002, Lee & Peale 2002, Kley et al. 2004). The planets subsequently migrate maintaining the commensurability. The capture into resonance of migrating planets in the earth mass range has also been studied (Papaloizou & Szuszkiewicz 2005, McNeil et al. 2005, Cresswell & Nelson 2006).

Once an embedded pair of planets is in resonance, the resonant angles (see below) and the angular difference of the apsidal lines are generally found to librate about fixed values. Note that the apsidal lines need not necessarily be aligned or anti-aligned. The relative orientation of the orbits may be phase-locked at an angle that differs from 0 or 180 deg, depending on their eccentricities and the mass of the planets (Beaugé et al. 2003, Kley et al. 2004).

In this paper, we study the commensurabilities that are established when a population of protoplanets with masses on the order of an earth mass migrate together through a protoplanetary disk. As they migrate, the planets undergo collisions which are assumed to result in mergers. This causes their masses to grow with time. We suppose that the protoplanetary disk has an inner edge interior to which is a cavity inside which disk-planet interactions and induced orbital migration cease. Observations suggest the existence of

magnetospheric cavities of this type with their extent controlled by the magnetic field of the central star (e.g., Bouvier et al. 2006). Inner disk boundaries in the range 0.05–0.1 au might be expected. Once the planets enter such a cavity, both additional collisions and mergers as well as tidal interaction with the star cause strict commensurability to be lost, although near-commensurability and locking of the apsidal lines of the orbits of pairs of planets may be maintained under the action of both these processes. Similar effects resulting from tidal interaction have been noted in the context of the solar system (e.g., Dermott et al. 1988) and in the context of extrasolar systems of giant planets (Novak et al. 2003). We now consider the dynamics of two planets in mean motion resonance, with locked apsidal lines, that are subject to tidal interaction with the central star that causes orbital circularization and show how strict commensurability is lost while the relative orientation of the apsidal lines can be maintained.

2.2. Loss of commensurability through tidal dissipation

Once a planet has migrated to small enough radii, tidal interaction with the central star becomes significant. If we assume that the rotation period of the central star is longer than the orbital period of the planet, which is expected for planets with orbital periods of ~ 4 days or less, tidal interaction between the star and the planet leads to eccentricity damping and orbital decay. The consequent reduction in semi-major axis would tend to cause any previously formed commensurability to be lost. Here we neglect the tides raised on the star by the planet, as we only consider planets of a few earth masses for which such tides are not expected to be significant (Goldreich & Soter 1966). To get some insight into the dynamics of the system, we consider a simple model in which there are only two planets orbiting a star of mass M_\star . We denote by m_i , a_i , e_i and n_i the mass, semi-major axis, eccentricity and mean motion of the inner planet ($i = 1$) and the outer planet ($i = 2$). The two planets are presumed to be in a mean motion resonance so that $n_1/n_2 = (p + q)/p$, where p and q are two integers. To simplify the discussion, we consider only the e_i^q -eccentricity resonances with $q = 1$. The associated resonant angles are $\Phi_1 = p\lambda_1 - (p + 1)\lambda_2 + \tilde{\omega}_1$ and $\Phi_2 = p\lambda_1 - (p + 1)\lambda_2 + \tilde{\omega}_2$ where, for ($i = 1, 2$), λ_i are the mean longitudes and $\tilde{\omega}_i$ are the arguments of pericentre.

The rates of change of the semi-major axes and eccentricities for planets $i = (1, 2)$ induced by the resonant interaction can be found from the following equations (e.g., Dermott et al. 1988):

$$\frac{da_i}{dt} = \frac{2}{m_i} \sqrt{\frac{a_i}{GM_\star}} \frac{\partial U}{\partial \lambda_i}, \quad (1)$$

$$\frac{de_i}{dt} = -\frac{1}{e_i m_i \sqrt{GM_\star a_i}} \frac{\partial U}{\partial \tilde{\omega}_i}. \quad (2)$$

The right hand side of equation (2) is written to lowest order in the eccentricities which are assumed to be small. Here, U is the interaction potential which, to first order in the eccentricities, is of the form:

$$U = -\frac{m_1 m_2}{a_2} [e_1 S_1(\alpha) \cos \Phi_1 + e_2 S_2(\alpha) \cos \Phi_2], \quad (3)$$

where $\alpha = a_1/a_2$ and the S_i are known functions (Goldreich 1965, Dermott et al. 1988), the detailed form of which does not affect our conclusions.

The rates of change of e_i and a_i also have additional contributions $(de_i/dt)_t$ and $(da_i/dt)_t$ arising from tidal dissipation (hereafter, the subscript 't' will denote variations due to tidal effects). Thus, by use of equations (1) and (3), we obtain:

$$\frac{da_1}{dt} = \frac{2p}{m_1} \sqrt{\frac{a_1}{GM_\star}} F + \left(\frac{da_1}{dt} \right)_t, \quad (4)$$

$$\frac{da_2}{dt} = -\frac{2(p+1)}{m_2} \sqrt{\frac{a_2}{GM_\star}} F + \left(\frac{da_2}{dt} \right)_t, \quad (5)$$

with:

$$F = \frac{m_1 m_2}{a_2} [e_1 S_1(\alpha) \sin \Phi_1 + e_2 S_2(\alpha) \sin \Phi_2]. \quad (6)$$

In addition, we find, from equations (2) and (3), for the rate of change of the eccentricities:

$$\frac{de_1}{dt} = -\frac{1}{e_1 m_1 \sqrt{GM_\star a_1}} F_1 + \left(\frac{de_1}{dt} \right)_t, \quad (7)$$

$$\frac{de_2}{dt} = -\frac{1}{e_2 m_2 \sqrt{GM_\star a_2}} F_2 + \left(\frac{de_2}{dt} \right)_t, \quad (8)$$

where:

$$F_i = \frac{m_1 m_2}{a_2} e_i S_i(\alpha) \sin \Phi_i, \quad (i = 1, 2) \quad (9)$$

and we have $F = F_1 + F_2$.

We are now going to show from the above equations that, if the resonance is maintained on average, the eccentricities must decrease with time. This means that the existence of the resonance acting through the two resonant angles cannot prevent the decay of the eccentricities due to the action of the tides. Indeed, for the resonance to be maintained on average, we must have $d \ln(a_1/a_2)/dt = 0$. Equations (4) and (5) then indicate that, on average:

$$\left[\frac{2p}{m_1 a_1} \sqrt{\frac{a_1}{GM_\star}} + \frac{2(p+1)}{m_2 a_2} \sqrt{\frac{a_2}{GM_\star}} \right] F = - \left[\frac{d \ln(a_1/a_2)}{dt} \right]_t. \quad (10)$$

We can now use equations (7) and (8) to obtain:

$$m_1 \sqrt{GM_\star a_1} \frac{de_1^2}{dt} + m_2 \sqrt{GM_\star a_2} \frac{de_2^2}{dt} = -2F + m_1 \sqrt{GM_\star a_1} \left(\frac{de_1^2}{dt} \right)_t + m_2 \sqrt{GM_\star a_2} \left(\frac{de_2^2}{dt} \right)_t. \quad (11)$$

Now, the effect of the tides causing circularization is to decrease e_i , i.e. $(de_i/dt)_t < 0$, while conserving the angular momentum of m_i . Thus a_i also decreases. But tides are stronger in m_1 , which is closer to the central star, which means that $[d \ln(a_1/a_2)/dt]_t < 0$. Equation (10) then implies that F is positive. It then follows that the right hand side of equation (11) is negative from which we can deduce that the eccentricities decrease with time as long as any one of them is non zero. This implies that if the resonance is maintained the e_i must ultimately decrease.

However, for the resonance to be maintained, one requires that the change in a_1 produced by tides in one libration period be much smaller than the amplitude of the oscillation in a_1 in resonance, Δa_1 (adiabatic criterion, see, e.g., Dermott et al. 1988). We are now going to show that this is not expected to be compatible with a decrease of the eccentricities. Indeed, when the eccentricity decreases, the libration period increases and Δa_1 decreases, so that at some point the resonance is broken. To see how this happens, as long as the eccentricities are not too small, one can use a perturbation scheme with small parameter $\epsilon = \sqrt{m_i/M_\star}$, where m_i is the largest of the planet masses. For resonance libration, we expect $d/dt = \mathcal{O}(\epsilon n_i)$. As $d\tilde{\omega}_i/dt = \mathcal{O}(\epsilon^2 n_i)$, to lowest order this is commonly neglected (Dermott et al. 1988). Under this scheme (which in addition requires $e_i \gg \epsilon^{2/3}$), the angles Φ_1 and Φ_2 obey the same equation (Dermott et al. 1988):

$$\frac{d\Phi_1}{dt} = \frac{d\Phi_2}{dt} = pn_1 - (p+1)n_2, \quad (12)$$

and $\Phi_1 - \Phi_2 = \tilde{\omega}_1 - \tilde{\omega}_2$ is constant. Thus we find:

$$\frac{d^2\Phi_1}{dt^2} = -\frac{3F}{\sqrt{GM_\star}} \left[\frac{p^2 n_1}{m_1 \sqrt{a_1}} + \frac{(p+1)^2 n_2}{m_2 \sqrt{a_2}} \right] + p \left(\frac{dn_1}{dt} \right)_t - (p+1) \left(\frac{dn_2}{dt} \right)_t. \quad (13)$$

This can be further reduced to a forced pendulum equation (e.g., Goldreich 1965):

$$\frac{d^2\xi}{dt^2} = -\omega_L^2 \sin \xi + p \left(\frac{dn_1}{dt} \right)_t - (p+1) \left(\frac{dn_2}{dt} \right)_t, \quad (14)$$

where $\xi = \Phi_1 - \delta$, with:

$$\tan \delta = \frac{e_2 S_2 \sin(\tilde{\omega}_1 - \tilde{\omega}_2)}{e_1 S_1 + e_2 S_2 \cos(\tilde{\omega}_1 - \tilde{\omega}_2)}, \quad (15)$$

and the libration frequency is given by:

$$\omega_L^2 = \frac{3m_1m_2}{\sqrt{GM_*a_2}} \left(\frac{p^2n_1}{m_1\sqrt{a_1}} + \frac{(p+1)^2n_2}{m_2\sqrt{a_2}} \right) \sqrt{e_1^2S_1^2 + e_2^2S_2^2 + 2e_1e_2S_1S_2 \cos(\tilde{\omega}_1 - \tilde{\omega}_2)}. \quad (16)$$

From adiabatic invariance, we conclude that as the eccentricities inevitably decrease because of circularization causing a decrease in libration frequency, the oscillation amplitude of $d\xi/dt$ decreases as do the excursions Δa_i while the amplitude of ξ itself increases. This naturally is expected to lead to the disruption of the resonance.

We have shown that for the resonance to be maintained the eccentricities have to decrease, and such a decrease of the eccentricities is expected to lead to the resonance being disrupted. Therefore, the resonance is not expected to be maintained under the action of tidal circularization. However, secular evolution of the semi-major axes occurring because of the circularization may cause other resonances to be approached with subsequent repetition of the disruption process discussed here.

Note that at the order we have worked above, $\Delta\tilde{\omega} = \tilde{\omega}_1 - \tilde{\omega}_2$ is constant, corresponding to a secular resonance for which apsidal alignment is maintained. As this type of resonance does not require a mean motion commensurability, it is possible for it to be maintained during the circularization process as well as some scattering and merger events (see below).

3. Model and initial conditions

We consider a system consisting of a primary star and N cores or protoplanets embedded in a gaseous disk surrounding it. The cores undergo gravitational interaction with each other and the star and are acted on by tidal torques from the disk.

Work by several authors (e.g., Kley et al. 2004; Papaloizou & Szuszkiewicz 2005; Cresswell & Nelson 2006) has demonstrated that the essential aspects of their motion can be captured by N -body integration. The effect of the disk torques and dissipative forces are included in the integration. Such a procedure has been shown to give results very similar to those obtained when the disk response induced by a planetary perturber and the torques acting back on the protoplanet are calculated using hydrodynamic simulations.

The equations of motion are:

$$\frac{d^2\mathbf{r}_i}{dt^2} = -\frac{GM_*\mathbf{r}_i}{|\mathbf{r}_i|^3} - \sum_{j=1 \neq i}^N \frac{Gm_j(\mathbf{r}_i - \mathbf{r}_j)}{|\mathbf{r}_i - \mathbf{r}_j|^3} - \mathbf{\Gamma} + \mathbf{\Gamma}_i + \mathbf{\Gamma}_r, \quad (17)$$

where M_\star , M_i and \mathbf{r}_i denote the mass of the central star, that of planet i and the position vector of planet i , respectively. The acceleration of the coordinate system based on the central star (indirect term) is:

$$\mathbf{\Gamma} = \sum_{j=1}^N \frac{Gm_j\mathbf{r}_j}{|\mathbf{r}_j|^3}, \quad (18)$$

and that due to tidal interaction with the disk and/or the star is dealt with through the addition of extra forces as in Papaloizou & Larwood (2000):

$$\mathbf{\Gamma}_i = -\frac{1}{t_{m,i}} \frac{d\mathbf{r}_i}{dt} - \frac{2}{|\mathbf{r}_i|^2 t_{e,i}} \left(\frac{d\mathbf{r}_i}{dt} \cdot \mathbf{r}_i \right) \mathbf{r}_i - \frac{2}{t_{i,i}} \left(\frac{d\mathbf{r}_i}{dt} \cdot \mathbf{e}_z \right) \mathbf{e}_z, \quad (19)$$

where $t_{m,i}$, $t_{e,i}$ and $t_{i,i}$ are the timescales over which, respectively, the angular momentum, the eccentricity and the inclination with respect to the unit normal \mathbf{e}_z to the gas disk midplane change. Evolution of the angular momentum and inclination is due to tidal interaction with the disk, whereas evolution of the eccentricity occurs due to both tidal interaction with the disk and the star. We have:

$$\frac{1}{t_{e,i}} = \frac{1}{t_{e,i}^d} + \frac{1}{t_{e,i}^s}, \quad (20)$$

where $t_{e,i}^d$ and $t_{e,i}^s$ are the contribution from the disk and tides raised by the star, respectively. Relativistic effects are included through $\mathbf{\Gamma}_r$ (see Papaloizou & Terquem 2001).

3.1. Orbital circularization due to tides from the central star

The circularization timescale due to tidal interaction with the star is given by Goldreich & Soter (1966) as:

$$t_{e,i}^s = 4.065 \times 10^4 \left(\frac{M_\oplus}{M_i} \right)^{2/3} \left(\frac{20a_i}{1 \text{ au}} \right)^{6.5} Q' \text{ years}, \quad (21)$$

where a_i is the semi-major axis of planet i . Here and below we have adopted unit density in cgs units for the planet. The parameter $Q' = 3Q/(2k_2)$, where Q is the tidal dissipation function and k_2 is the Love number. For solar system planets in the terrestrial mass range, Goldreich & Soter (1966) give estimates for Q in the range range 10–500 and $k_2 \sim 0.3$. The values of these quantities are clearly very uncertain under the very different physical conditions likely to be appropriate to extrasolar planets. We have performed simulations with $Q' = 10, 100$ and 1000. In the first case, tidal circularization is very effective, while in the last it only produces very small effects over practical simulation times.

For a 1 earth mass planet at 0.05 au and $Q' = 100$, we get $t_{e,i}^s = 4 \times 10^6$ years, whereas at 0.1 au and for $Q' = 1000$, we get $t_{e,i}^s = 4 \times 10^9$ years. Thus a range of circularization timescales going from short compared to the formation time to comparable to the age of the system may apply.

3.2. Type I migration

In the local treatment of type I migration (e.g., Tanaka et al. 2002), if the planet is not in contact with the disk, there is no interaction between them so that $t_{m,i}$, $t_{e,i}^d$ and $t_{i,i}$ are taken to be infinite. When the planet is in contact with the disk, disk–planet interactions occur leading to orbital migration as well as eccentricity and inclination damping (e.g., Ward 1997). In that case, away from the disk edge, we adopt:

$$t_{m,i} = 146.0 \left[1 + \left(\frac{e_i}{1.3H/r} \right)^5 \right] \left[1 - \left(\frac{e_i}{1.1H/r} \right)^4 \right]^{-1} \left(\frac{H/r}{0.05} \right)^2 \frac{M_\odot}{M_d} \frac{M_\oplus}{M_i} \frac{a_i}{1 \text{ au}} \text{ years}, \quad (22)$$

$$t_{e,i}^d = 0.362 \left[1 + 0.25 \left(\frac{e_i}{H/r} \right)^3 \right] \left(\frac{H/r}{0.05} \right)^4 \frac{M_\odot}{M_d} \frac{M_\oplus}{M_i} \frac{a_i}{1 \text{ au}} \text{ years}, \quad (23)$$

and $t_{i,i} = t_{e,i}$ (eq. [31] and [32] of Papaloizou & Larwood 2000 with $f_s = 0.6$). Here e_i is the eccentricity of planet i , H/r is the disk aspect ratio and M_d is the disk mass contained within 5 au. We have assumed here that the disk surface mass density varies like $r^{-3/2}$. For a 1 earth mass planet on a quasi-circular orbit at 1 au, we get $t_{m,i} \sim 10^5$ yr and $t_{e,i} \sim 500$ yr for $M_d = 10^{-3} M_\odot$ and $H/r = 0.05$. Note that the timescales given by equations (22) and (23) can be used not only for small values of e_i , but also for eccentricities larger than H/r . The eccentricity dependence of these timescales is supported by the simulations of Cresswell & Nelson (2006). Their absolute normalization can be varied by scaling the disk surface density. We have checked that the general simulation outcomes are robust to varying the ratio $t_{e,i}^d/t_{m,i}$ by a factor of three.

3.3. Corotation torques

Type I migration as discussed above is caused through the excitation of density waves at Lindblad resonances. However, torques due to corotation resonances may also act. These depend on the gradient of specific vorticity or vortensity (Goldreich & Tremaine 1979). They are generally small, actually vanishing in a keplerian disk with a surface density profile

$\propto r^{-3/2}$, except where the surface density varies fairly rapidly. Based on a three dimensional linear response calculation, for a planet on a circular orbit and disk surface density $\Sigma \propto r^{-\alpha}$, Tanaka et al. (2002) find that migration stops for $\alpha = -27/11$ and is outward for surface density profiles that decrease more rapidly inwards.

In our simulations, for simplicity, we have either adopted equations (22) and (23) with no interaction interior to the disk inner edge, which from the above discussion we expect to correspond to a moderate taper with $\alpha = -27/11$, or allowed for a very sharp edge as described below.

Recently, Masset et al. (2006) have proposed that inward protoplanet migration can be halted near sharp disk inner edges which act as traps. Here we study the migration of protoplanets into an inner evacuated cavity so we thus consider the possibility of corotation torques produced in a narrow region near the disk inner cavity boundary. We comment that the calculation of corotation torques is very uncertain, being dependent not only on the details of the edge profile, but also on the degree of resonance saturation which itself depends on the amount of turbulence and viscosity present (Masset et al. 2006). We here point out two possible effects that may act to reduce the effectiveness of such edge torques when there is a system of interacting planets. The first is planet–planet scattering, which could move the semi–major axis of a planet across the edge. The second is that protoplanets on eccentric orbits will only sample the edge for a fraction of the orbit and accordingly suffer a reduced torque. Note that orbital eccentricity is more likely to be sustained when the protoplanet orbit is only partly contained within the disk as then the effectiveness of disk damping is reduced.

Corotation torques can act to produce outward torques in the inner edge domain $R_{in} - \Delta_r/2 < r < R_{in} + \Delta_r/2$, where the surface density changes rapidly. Here the edge is centered on $r = R_{in}$ and the total width of the domain is Δ_r . As in the case of Lindblad torques, the effect of orbital eccentricity is to reduce such corotation torques and this effect has been incorporated in our modelling.

Masset et al. (2006) indicate that when $a_i = R_{in}$, outward corotation torques may exceed the normal inward type I torques by a factor of five when $e = 0$. To investigate the possible role of such torques, in some of our simulations we adopted the following approximate procedure. In the edge domain, we replaced $t_{m,i}$ by $-0.2t_{m,i,0}(1+e_i r/H)$, where $t_{m,i,0}$ denotes $t_{m,i}$ evaluated for $e_i = 0$. The factor in brackets accounts for the fact that for large e_i , the effective values of the azimuthal number m contributing to the corotation torque are reduced by a factor $H/(re_i)$. In practice, this detail is not important for the simulations we carried out, because e_i never significantly exceeds H/r in these cases. Thus a planet in the center of the domain with $e_i = 0$ experiences an outward torque of the required magnitude, while for

larger e_i the time averaged torque will decline through the factor $[H/(re_i)][\Delta_r/(2re_i)]$. The second factor here estimates the fractional reduction of the time spent in the edge domain once $e_i > \Delta_r/(2R_{in})$.

Although we have focussed on the reversed edge torque as being due to a corotation effect, it is possible that similar features could be produced by, e.g., the presence of a toroidal magnetic field near the inner edge (Terquem 2003).

3.4. Numerical integration and initial conditions

The equations of motion are integrated using the Bulirsch–Stoer method (e.g., Press et al. 1993). All the planets are supposed to have an identical mass density $\rho = 1 \text{ g cm}^{-3}$. If the distance between planets i and j becomes less than $[3M_i/(4\pi\rho)]^{1/3} + [3M_j/(4\pi\rho)]^{1/3}$, a collision occurs and as is commonly assumed in studies of this kind, the planets are assumed to merge. They are subsequently replaced by a single planet of mass $M_i + M_j$ which is given the position and the velocity of the center of mass of planets i and j .

The simulations begin by placing N planets on coplanar orbits in an annulus with outer and inner radii r_{out} and $r_{in} = xr_{out}$, respectively. In some cases, the planets $i = 1, 2, \dots, N$ were given the radial coordinate $r = r_{in}[1 + (x^{-3} - 1)/(3i - 2)]^{1/3}$ together with the polar angle $\varphi = 2\pi/i$. In other cases, r and φ were chosen randomly. The planets were then given the local circular velocity in the azimuthal direction. We have fixed $r_{out} = 1$ or 2 au and $x = 0.1$. Note that the range of radii over which the cores are initially spread does not affect the outcome of the simulations. Indeed, if r_{out} were larger, the cores would just take longer to migrate in. The disk is supposed to be truncated at some inner edge radius R_{in} in the neighborhood of which a corotation torque may apply.

Initially, all the planets have the same mass M_p . We have fixed $M_p = 0.1 M_{\oplus}$ or $M_p = 1 M_{\oplus}$. This range of masses has been chosen because they have expected migration times from 5 au to the central regions of the disk that are comparable to disk lifetimes. Cores more massive than $1 M_{\oplus}$ can subsequently form through mergers. We investigate what final systems of planets may be produced interior to the disk inner boundary.

Time $t = 0$ marks the beginning of the simulations. It corresponds to the time when the cores considered begin to migrate from the initial positions allocated to them. As it takes at least close to a million years to form these cores, $t = 0$ for the scenario envisaged here should correspond to a time when the disk has already evolved significantly. Note that some cores may have begun to form further away from the central star than the initial positions allocated to them. Here we assume that we can take $t = 0$ to be the time at which

all cores formed in the disk that are able to migrate down to the inner cavity within the disk lifetime are contained within the radius r_{out} of the initial distribution. The total mass contained in these cores is varied between 1 and 25 earth masses. We comment that both increasing r_{out} or decreasing the initial core mass have the effect of extending the evolution time, that being inversely proportional to the core mass. Simulations performed with either larger r_{out} such as A2, A9, B3, or initial core masses reduced by a factor of ten such as A10, indicated below, produce qualitatively similar end results but with correspondingly reduced final total masses in the latter case. This is indicative that drawing out the evolution time does not alter the qualitative behavior.

4. Numerical results

For the runs presented here, we fixed $M_\star = 1 M_\odot$, $H/r = 0.05$ and $M_d = 10^{-3} M_\odot$. The prescriptions for disk planet torques, eccentricity and inclination damping rates were, apart from possible modifications listed in table 1, as described in section 3. With these parameters specified, the quantities characterizing a run were the initial number of planetary cores, N , their initial mass, M_p , the tidal dissipation parameter, Q' , the radius of the inner disk edge, R_{in} , and the bounding radii of the initial planet distribution, r_{in} and r_{out} . Table 1 lists the parameters corresponding to the different runs. The initial number of planets N is either 10, 12 or 25. The outer radius of the initial distribution, r_{out} , is either 1 or 2 au.

4.1. General outcome

All the runs start with the same qualitative evolution. A few collisions and mergers take place very close to the beginning of the simulation before significant migration occurs. These result from the initial unstable distribution of orbits. Then as the planets migrate inwards, further collisions and mergers occur on a timescale somewhat shorter than the complete migration timescale. Finally the runs end with a stable configuration with a few planets, typically between 2 and 5, which will be inside the inner cavity when no edge corotation torques are applied. In that case, the most massive planets tend to be on the tightest orbits, as they migrate faster. Mean motion resonances are always established during the migrating phase. Some rearrangement may take place as the planets approach the inner cavity and further collisions occur, but by the time all the planets left over finally enter the cavity, mean motion resonances between almost all pairs of planets have been established. At that stage, residual scattering/mergers, should they occur, together with tidal interaction with the central star leading to circularization of the orbits, on a timescale which is shorter for

closer in planets, results in the disruption of strict commensurabilities (see section 2.2). The semi-major axes usually do not evolve very significantly however, so the mean motions can stay near commensurate.

We now describe in more detail run A3, which is a typical run. It begins with $N = 12$ planets each having a mass $M_p = 1 M_\oplus$ and for which $r_{\text{out}} = 1$ au and $R_{\text{in}} = 0.05$ au. The time evolution of the semi-major axes and eccentricities of the planets up to 3×10^5 years is shown in figure 1. Within the first 100 years after the start of the calculation, before any migration has occurred, 5 pairs of planets merge. Another merger occurs after $\sim 10^4$ years. After $\sim 2 \times 10^4$ years, the 4 innermost planets enter the inner cavity, where their semi-major axes do not evolve anymore. When one of the planets still in the disk finally approaches the inner cavity, after $\sim 3 \times 10^4$ years, it pumps up the eccentricity of the innermost planets which results in 2 pairs of planets undergoing collisions and mergers. At that point, 3 planets are left in the cavity, where they are joined after $\sim 7 \times 10^4$ years by the outermost planet. Pairs of orbits are then in mean motion resonances. Subsequent tidal circularization, that acts on a timescale of a few millions years and is seen on the bottom panel of figure 1, will disrupt the resonances, but the orbits may stay nearly commensurate.

To study the action of tidal circularization on a commensurability formed by disk planet interaction, for purely illustrative purposes we consider a simple example with two planets. In the notation of section 2.2, these had masses $m_1 = 2 M_\oplus$ and $m_2 = 8 M_\oplus$. We performed two simulations with the same disk parameters as A3 but, for practical reasons, the circularization rates were taken to be ten and a hundred times faster. Comparison of these cases indicates that the form of the evolution is the same but with the time scale appropriately stretched. These planets initially migrated into the inner cavity and formed a 5:4 commensurability for which the resonant angle $\Phi \equiv -\Phi_1 = 5\lambda_2 - 4\lambda_1 - \varpi_1$ has a small libration about zero. The subsequent evolution under the action of orbital circularization is shown in figure 3. As expected, the libration amplitude increases as the planets begin to move out of the 5:4 resonance. In the case with faster circularization, the angle Φ eventually begins to show circulation with the 4:3 resonance being approached. In this particular example, the eccentricity attains very small values ≤ 0.001 while away from the center of resonances. The indication is that the system separates as it moves away from resonant configurations associated with high eccentricities.

For run A3, the 4 planets left at the end of the run, that we label 'A', 'B', 'C' and 'D', have a mass of 2, 6, 3 and $1 M_\oplus$, respectively. The two innermost planets, A and B, are in a 3:2 mean motion resonance, with $|n_A/n_B - 3/2| \sim 10^{-3}$, where n_A and n_B are the mean motions of planets A and B, respectively. In figure 2 we plot the angular difference of the apsidal lines $\Delta\tilde{\omega}$ and the resonant angle $\Phi = 3\lambda_B - 2\lambda_A - \tilde{\omega}_A$, where λ_A and λ_B are

the mean longitudes of planets A and B, respectively, and $\tilde{\omega}_A$ is the argument of pericentre of planet A. After $\sim 10^5$ years, both $\Delta\tilde{\omega}$ and Φ librate about some fixed values (344 and 207 deg, respectively) with an amplitude of a few degrees, which indicates apsidal locking and mean motion resonance. Note that $\Delta\tilde{\omega}$ and Φ do not necessarily librate about 0 or 180 deg when there is a mean motion resonance. As shown by Beaugé et al. (2003), the equilibrium value of these angles tend to depart from either 0 or 180 deg when the eccentricity of the planets is not small (typically higher than ~ 0.1).

We have run a case with a lower total mass (A10, $N = 10$ and $M_p=0.1 M_\oplus$) and a case with a higher total mass (A11, $N = 25$ and $M_p=1 M_\oplus$). The results of these runs are similar to those described above, only the mass of the planets left in the inner cavity changes, roughly scaling with the initial total mass.

In the run A3 described above, we found that $\Delta\tilde{\omega}$ and Φ were librating about some fixed values. Note that this is not always the case. In some of the runs we have performed, these angles circulate, so that the systems are not formally exactly commensurable. We also point out that the commensurabilities given in table 1 are accurate to within at least 1%, and often to within 0.1%.

4.2. Tidal circularization

To investigate the effect of changing the orbital circularization rate, we performed simulations A8 with $Q' = 10$ and B2 with $Q' = 1000$. Both these runs have inner cavity radius $R_{\text{in}} = 0.1$ au. In the former case, orbital circularization is manifest in the simulation, while in the latter case, it is too long to be manifest.

The simulation A8 ended with three planets in the inner cavity in near but not exact commensurability. The evolution of the semi-major axes is shown in figure 4 as is the evolution of the angular differences of the apsidal lines $\Delta\tilde{\omega}$ for the two innermost planets and the innermost and outermost of the three planets. These librate about alignment in the former case and anti-alignment in the latter case. In figure 5, the evolution of the semi-major axes is shown for run B2. The right panel of this figure shows the evolution of the angular difference of the apsidal lines for the two planets which remain in the inner cavity. This oscillates around the anti-aligned position. This case has a very long circularization time. It is possible that for some of these cases with larger cavity radii, some orbital eccentricity remains on 10^9 years timescales, in which case the alignment/anti-alignment of the apsidal lines could be observed. The evolution of the eccentricities in the simulations B2 and A8 is shown in figure 6. In the latter case, a small amount decay for the innermost planets can be

seen, while in the former, the circularization rate due to tides induced by the central star is too small to have any effect.

We also performed simulation B1 which had identical parameters to A8 but inner cavity radius $R_{\text{in}} = 0.05$ au and simulation B3 which was identical to B2 apart from the size of the initial domain in which the planets were started. In both simulations, the number of remaining planets and final period ratios were similar.

4.3. Migration halted at the disk inner edge by corotation torques

In the runs presented above, the interaction between the planets and the disk leads to inward migration of the planets. After a planet enters the inner cavity, it is no longer pushed in by the disk, but it can still be pushed in by planets further away which enter the cavity at a subsequent time. Note that when a planet approaches the inner cavity, it may gently push in the planets which are already inside, but it may also perturb them in such a way that a merger occurs. Both processes are seen in the run A3 displayed in figure 1.

It has been argued recently (Masset et al. 2006) that when an embedded planet reaches a region of the disk where the mass density decreases sharply, the tidal torque from the disk is reversed so that migration is halted and the planet is trapped at this location. We have performed runs in which the torque at the inner edge of the disk is reversed according to the prescription described in section 3.3 to test whether planets penetrate inside the cavity. In simulations C1, C2 and C3, such torques were applied. The boundary torques that we applied were strong enough to prevent entry into the inner cavity while the disk was present. We emphasize that this is the important feature of the torque prescription that we adopted and that otherwise results should be independent of details.

We considered two phases in these cases for which the disk edge torque prevented entry into the inner cavity. While embedded in the disk, the strong orbital circularization allowed close commensurabilities to form among six to seven planets in a similar manner to that described for simulation A3. These are indicated in table 1. A state was reached for which the semi-major axes became almost constant such that angular momentum transferred from inner to outer planets prevented their inward migration. After this state was reached, the disk was removed (by setting the induced migration and circularization rates to zero) in order to study the further evolution and in particular the effect of removing the stabilizing influence of disk eccentricity damping.

Simulation C3 had $Q' = 1000$ and the larger inner cavity radius $R_{\text{in}} = 0.1$ au. The evolution of the semi-major axes and eccentricity of the outermost planet are shown in

figure 7. As indicated in table 1, this run produced a system of six planets stably locked in a series of commensurabilities (9:8, 4:3, 7:6, 7:6, 5:4). In this state, the negative torques acting on the outer planets were effectively balanced by the corotation torque acting on the innermost planet so that evolution of the semi-major axes ceased. The disk was removed at time 1.32×10^5 years. Shortly after that time, two of the planets merged leaving a system of somewhat more widely spaced five planets that survived with almost constant semi-major axes (see figure 7). The period ratios moving outwards were then (1.125, 1.44, 1.25, 1.26). The stability of systems of low mass planets has been considered by Chambers et al. (1996). They considered systems of three objects which in our case would correspond to $3 M_{\oplus}$ planets for up to $\sim 10^7$ inner orbits, and we have evolved our systems for similar or longer times. They found that the systems must be more widely separated to ensure stability for longer times. This is of course a statistical statement, there are no guarantees in specific cases. We also note the additional potential stabilisation provided by orbital circularization in our case. Nonetheless, if one makes the very arbitrary assumption that their results can be simply extrapolated to $\sim 10^{11}$ inner orbits, which would correspond to Gyr time scales, period ratios of ~ 1.25 would be required. This corresponds to a spacing between planets of 10.75 Hill radii. This is similar to what our systems show except that, in the case of run C3, the innermost pair are very close to a 9:8 commensurability. Although these two planets maintained locked apsides, the appropriate resonant angle Φ showed long term variations but did not librate. It is possible that some of the planets in such systems could later merge, forming a more widely separated system with fewer planets, but the general character is likely to be preserved. Simulations C1 and C2, which had smaller inner cavity radii, led to similar configurations while the disk was present. However, in these cases, the systems remained stable when the disk was removed. This may be because of the increased importance of orbital circulation, especially in the case of C2 which had seven remaining planets. In this case, with $Q' = 10$, orbital circularization cannot be neglected in the simulation run time and might be expected to assist system stability by preventing the slow build up of orbital eccentricities that could result in orbit crossing.

5. Summary and Discussion

We have calculated the evolution of a population of cores/planets with masses in the range $0.1\text{--}1 M_{\oplus}$ embedded in a disk. They evolve due to gravitational interaction with the central star, mutual gravitational interactions, tidal interaction with the disk and the star. Mutual interactions lead to orbit crossing and mergers, so that the cores grow during their evolution. Interaction with the disk leads to orbital migration. As cores with different masses and at different locations migrate with different rates, they capture each other in

mean motion resonances. Such captures enable planets to migrate inside the cavity interior to the disk inner edge. As they approach closer to the central star, for small enough cavities their orbits are circularized through tidal dissipation and strict commensurabilities are lost. That process may be also aided by scatterings and mergers of planets on unstable orbits that occur interior to the disk inner edge. Near-commensurability however may be maintained. Note too that if apsidal locking is established during migration, it can be preserved through the operation of these processes. All the simulations end with a population of typically between two and five planets, with masses depending on the initial mass. Note that the disk tidal torque may be reversed near the disk inner edge. When this is the case, although it is possible that some planets can still penetrate inside the cavity due to scatterings and/or weakening of the torques because of a finite eccentricity, some planets may be left in the disk, just beyond the inner edge, until that disperses.

The qualitative results do not depend on the detail of the initial conditions. As long as a population of cores is able to migrate inwards at different rates, the system evolves toward a family of a few planets which are almost always on near-commensurate orbits.

The orbital migration and eccentricity damping timescales we have adopted in this paper have been derived for type I migration in inviscid disks. Note that type I migration has been shown to follow a random walk in a turbulent disk (Nelson & Papaloizou 2004). The studies done in the present paper assume that the cores can migrate down to the disk inner edge, in regions where the gas is ionized and magnetic turbulence can develop (Fromang et al. 2002). These studies would of course not apply if there were no systematic inwards migration of the cores/protoplanets of the type we consider here. As of today, there is no indication that type I migration in a turbulent disk has a systematic trend (Nelson 2005), but this cannot be ruled out either. It is likely that type I migration does depend at least to some extent on the torque exerted by the material that corotates with the planet, which so far has not been taken into account in the simulations, which lack the required resolution. If there is a systematic trend, as long as the time averaged migration rate is inwards, by the averaging principle and as confirmed in test studies, short term fluctuations do not qualitatively change the results we have presented in this paper.

It has very recently been suggested (Paardekooper & Mellema 2006) that, because of effects arising from radiation trapping, type I migration in an optically thick laminar disk could be outward. This result, should it be confirmed for both laminar and turbulent disks, suggests that cores would not migrate inwards in the disk inner parts as long as the dust opacity is high enough there. However, after the dust settles and agglomerates to form cores, the opacity decreases and migration could then resume. It is indeed an observational fact that the disk inner parts (whithin a few au) become optically thin before the rest of the disk

is depleted.

The calculations done in this paper show that if hot super-Earths or Neptunes form by mergers of inwardly migrating cores, then such planets are most likely not isolated. We would expect to always find at least one, more likely a few, companions on close and often near-resonant orbits. To test this hypothesis, it would be of interest to look for planets of a few to ~ 10 earth masses in systems where hot super-Earths or Neptunes have already been found and there is no destabilizing influence of a giant planet close by.

It has been speculated that the cores of giant planets could form in a way similar to that investigated here, by accumulation of cores in the disk inner parts (e.g., Papaloizou & Terquem 1999). The calculations presented in this paper suggest that to assemble a massive core in the inner disk, significantly more mass in smaller cores may be needed to begin with. Indeed, most of the simulations end with at least three planets, and not with a single planet containing all the initial mass.

REFERENCES

- Beaulieu, J. P., et al., 2006, *Nature*, 439, 437
- Beaugé, C.; Ferraz-Mello, S.; Michtchenko, T. A., 2003, *ApJ*, 593
- Boss, A. P., 2000, *ApJ*, 536, L101
- Boss, A. P., 2006, *ApJ*, 644, L79
- Bouvier, J., Alencar, S. H. P., Harries, T. J., Johns-Krull, C. M., Romanova, M. M., 2006, in *Protostars and Planets V*, eds
- Brunini, A., Cionco, R. G., 2005, *Icarus*, , 177, 264
- Lin, D. N. C., Papaloizou, J. C. B., Terquem, C., Bryden, G., Ida, S., 2000, in *Protostars and Planets IV*, eds V. Mannings, A. P. Boss, S. S. Russell (Tucson: Univ. Arizona Press), p. 1111
- Chambers, J. E., Wetherill, G. W., Boss, A. P., 1996, *Icarus*, , 119, 261.
- Cresswell, P., Nelson, R. P., 2006, *A&A*, , 450, 833
- Dermott, S. F., Malhotra, R., Murray, C. D., 1988, *Icarus*, ,76, 295
- Fischer, D. A., Marcy, G. W., Butler, R. P., Vogt, S. S., Frink, S., Apps, K., 2001, *ApJ*, 551, 1107

- Fromang, S., Terquem, C., Balbus, S. A., 2002, *MNRAS*, , 329, 18
- Goldreich, P., 1965, *MNRAS*, , 130, 159
- Goldreich, P., Soter, S., 1966, *Icarus*, ,5 ,375
- Goldreich, P., Tremaine, S., 1979, *ApJ*, 233, 857
- Greenberg, R. J., Counselman, C. C., III, Shapiro, I. I., 1972, *Sci*, , 178, 747
- Greenberg, R., 1973, *AJ*, 78, 338
- Haisch K. E., Jr., Lada E. A., & Lada C. J., 2001, *ApJ*, 553, L153
- Haghighipour, N., 1999, *MNRAS*, , 304, 185
- Kley, W., 2000, *MNRAS*, , 313, L47
- Kley, W., Peitz, J., Bryden, G., 2004, *A&A*, , 735
- Lee, M. H., Peale, S. J., 2002, *ApJ*, 567, 596
- Masset, F., Snellgrove, M., 2001, *MNRAS*, , 320, L55.
- Masset, F. S., Morbidelli, A., Crida, A., Ferreira, J., 2006, *ApJ*, 642, 478
- Masunaga, H., Inutsuka, S., 1999, *ApJ*, 510, 822
- McNeil D., Duncan M., Levison H. F., 2005, *AJ*, 130, 2884
- Melita, M. D.; Woolfson, M. M., 1996, *MNRAS*, , 280, 854
- Mizuno, H., 1980, *Prog. Theor. Phys.*, 64, 544
- Murray, C. D., Dermott, S. F., 1999, *Solar System Dynamics (CUP)*, p. 254–255
- Nelson, R. P., 2005, *A&A*, , 443, 1067
- Nelson, R. P., Papaloizou, J. C. B., 2002, *MNRAS*, , 333, L26
- Nelson, R. P., Papaloizou, J. C. B., 2004, *MNRAS*, , 350, 849
- Nelson, R. P., Papaloizou, J. C. B., Masset, F. S., Kley, W., 2000, *MNRAS*, , 318,18
- Novak, G. S., Lai, D., Lin, D. N. C., 2003, *ASPC*, 294, 177
- Papaloizou, J. C. B., Larwood, J. D., 2000, *MNRAS*, , 315, 823

- Papaloizou, J. C. B., Szuszkiewicz, E., 2005, *MNRAS*, , 363, 153
- Papaloizou, J.C.B., Terquem, C., 2001, *MNRAS*, , 325, 221
- Papaloizou, J.C.B., Terquem, C., 2006, *RPPh*, 69, 119
- Paardekooper, S.-J., Mellema, G., 2006, astro-ph/0608658
- Press, W. H., Teukolsky, S. A., Vetterling, W. T., Flannery, B. P., 1993, *Numerical Recipes in FORTRAN* (CUP)
- Rivera, E. J., Lissauer, J. J., Butler, R. P., Marcy, G. W., Vogt, S. S., Fischer, D. A., Brown, T. M., Laughlin, G., Henry, G. W., 2005, *ApJ*, 634, 625
- Roy, A. E., 1978, *Orbital Motion* (Adam Hilger, Bristol), p. 280
- Snellgrove, M. D.; Papaloizou, J. C. B.; Nelson, R. P., 2001, *A&A*, , 374, 1092
- Tanaka, H., Takeuchi, T., Ward, W. R., 2002 *ApJ*, 565, 1257
- Terquem, C. E. J. M. L. J., 2003, *MNRAS*, , 341, 1157
- Ward, W.R., 1997, *Icarus*, , 126, 261

Run	N	M_p	Q'	R_{in}	r_{in}	r_{out}	Final masses	Final period ratios
A1	10	1	100	0.05	0.1	1	4, 2, 3, 1	3:2, 4:3, 6:5
A2	10	1	100	0.05	0.2	2	3, 6, 1	4:3, 7:5
A3	12	1	100	0.05	0.1	1	2, 6, 3, 1	3:2, 4:3, 6:5
A4	12	1	100	0.05	0.1	1	2, 6, 4	4:3, 3:2
A5	10	1	10	0.05	0.1	1	9, 1	2:1
A6	10	1	1000	0.05	0.1	1	8, 1, 1	1.46, 1.69
A7	10	1	1000	0.1	0.1	1	8, 2	1.42
A8	10	1	10	0.1	0.1	1	6, 3, 1	4:3, 6:5
A9	10	1	1000	0.1	0.2	2	5, 5	1.86
A10	10	0.1	100	0.05	0.1	1	0.9, 0.1	7:5
A11	25	1	100	0.05	0.1	1	12, 9, 4	2:1, 11:8
B1	10	1	10	0.05	0.1	1	3, 6, 1	1.37, 5:4
B2	10	1	1000	0.1	0.1	1	4, 6	1.37
B3	10	1	1000	0.1	0.2	2	3, 7	1.37
C1	10	1	1000	0.05	0.1	1	(3, 3, 1, 1, 1, 1) 3, 3, 1, 1, 1, 1	(7:6, 4:3, 6:5, 5:4, 5:4) 7:6, 4:3, 6:5, 5:4, 5:4
C2	10	1	10	0.05	0.1	1	(3, 2, 1, 1, 1, 1, 1) 3, 2, 1, 1, 1, 1, 1	(6:5, 6:5, 5:4, 6:5, 6:5, 5:4) 6:5, 6:5, 5:4, 6:5, 6:5, 5:4
C3	10	1	1000	0.1	0.1	1	(3, 3, 1, 1, 1, 1) 3, 3, 2, 1, 1	(9:8, 4:3, 7:6, 7:6, 5:4) 9:8, 1.44, 5:4, 1.26

Table 1: This table lists the parameters for each simulation. The label A denotes standard runs as described in section 3, the label B indicates that the disk eccentricity damping rates were decreased by a factor of three, the label C denotes that edge corotation torques were applied. N is the initial number of planets, M_p is their mass in units of M_{\oplus} , Q' is the tidal dissipation parameter, R_{in} is the radius of the disk inner edge (in au), r_{in} and r_{out} are the bounding radii of the initial planet distribution (in au). The table also lists the final masses (in units of M_{\oplus}) of the objects left at the end of the run from the innermost to the outermost planet and the period ratios for neighboring final objects starting from the innermost. In the case of runs labelled C, masses and period ratios at the stage when the planets reached a steady configuration while embedded in the disk are indicated in brackets. Values subsequently attained after disk removal are given on the lines below. Indicated mean motion commensurabilities apply to within one percent.

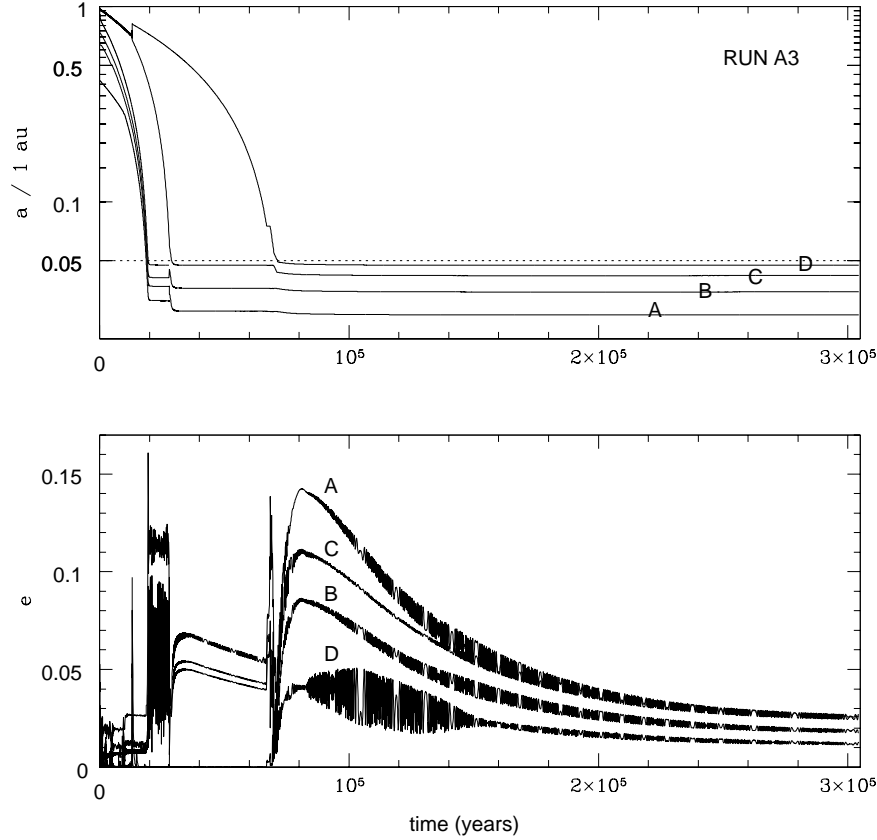


Fig. 1.— Evolution of the semi-major axes (in units of au and in logarithmic scale; *upper plot*) and of the eccentricity (*lower plot*) of the 12 planets in the system versus time (in units of years) for run A3. The solid lines correspond to the different planets, each having an initial mass of $1 M_{\oplus}$. In this and other similar figures, a line terminates just prior to a collision. On the upper plot, the dotted line indicates the location of the inner cavity ($R_{\text{in}} = 0.05$ au here). The letters label the different planets left after collisions have occurred. The mass of planets A, B, C and D is 2, 6, 3 and $1 M_{\oplus}$, respectively. Planets A and B, B and C, and C and D are in 3:2, 4:3, 6:5 mean motion resonances, respectively.

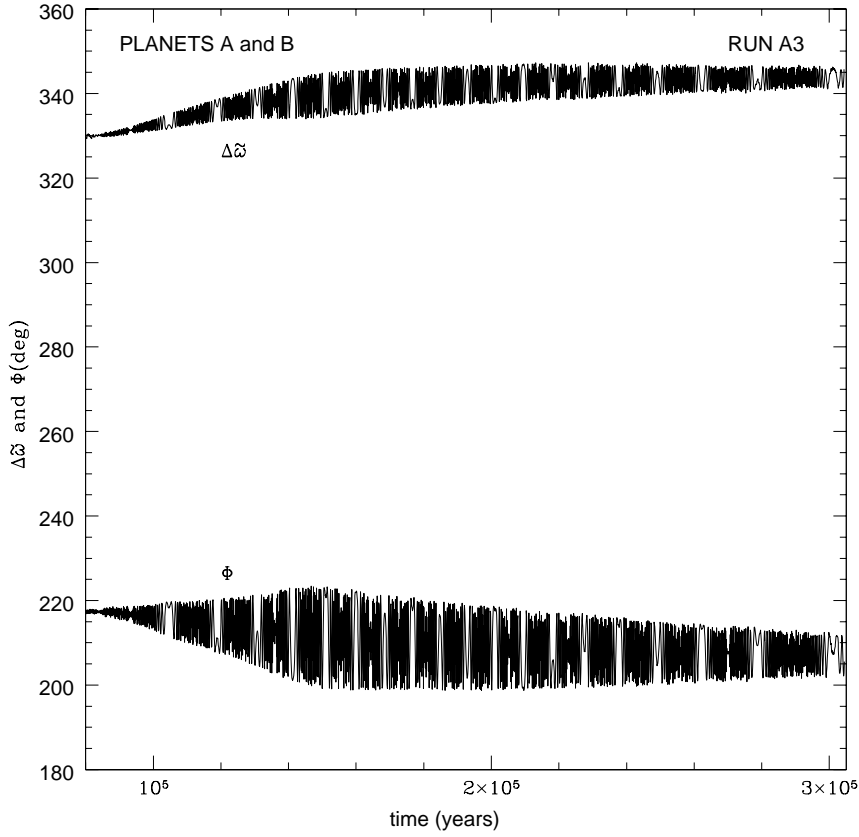


Fig. 2.— Evolution of the angular difference of the apsidal lines $\Delta\tilde{\omega}$ and of the resonant angle Φ (in degrees) for planets A and B versus time (in years), starting at 8×10^4 years after the beginning of the simulation, for the same run as in figure 1. The angles librate about some fixed values with an amplitude of a few degrees, which indicates mean motion resonance (3:2 here) and apsidal locking.

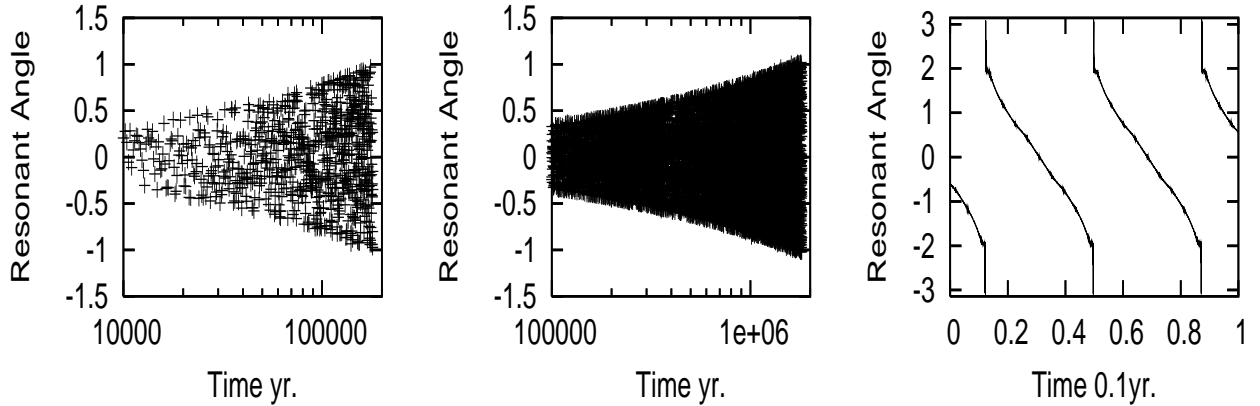


Fig. 3.— Evolution of the resonant angle $\Phi \equiv -\Phi_1 = 5\lambda_2 - 4\lambda_1 - \varpi_1$ expressed in radians for two interacting planets that disk interaction caused to enter a 5:4 resonance under the action of orbital circularization. The left panel is for a case with circularization rate 10 times faster than that illustrated in the middle panel. Both panels show the early stages of the evolution during which the libration amplitude increases as the planets begin to move out of the 5:4 resonance. Note that the evolution illustrated in the middle panel is ten times slower than that illustrated in the left panel, showing that the evolution is driven by the orbital circularization. In the case with faster circularization, the angle Φ begins to show circulation after a time $\sim 7 \times 10^5$ yr, as the system moves towards the 4:3 resonance. The right hand panel shows this circulation in a high time resolution plot taken after $\sim 7.4 \times 10^5$ yr. The circulation period ~ 12 days, while the orbital period of the inner planet ~ 3 days.

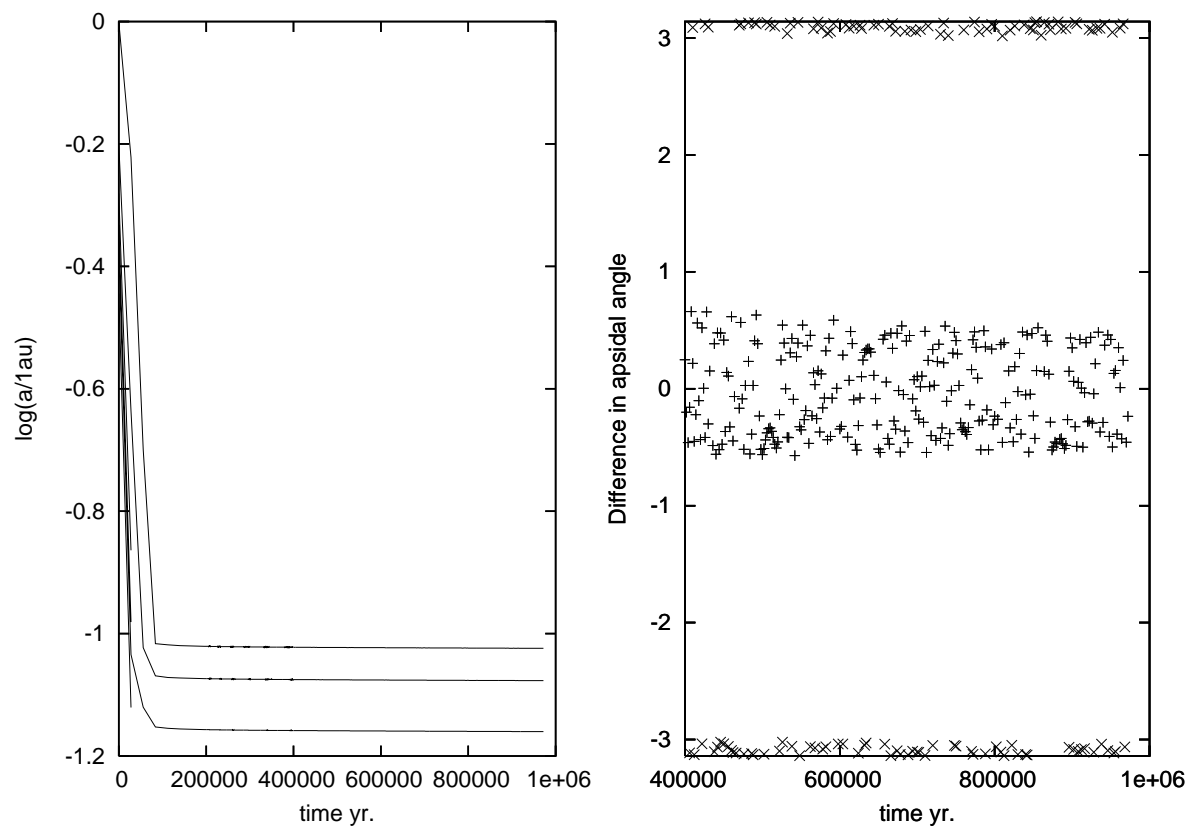


Fig. 4.— The left panel shows, as in figure 1, the evolution of the semi-major axes for run A8. The right panel shows the evolution of the angular differences of the apsidal lines $\Delta\tilde{\omega}$ (in radians) for the two innermost, according to semi-major axis, planets (points clustered about 0) and the innermost and outermost of the three planets (points clustered about π and $-\pi$). Note that because of periodicity any multiple of 2π can be added.

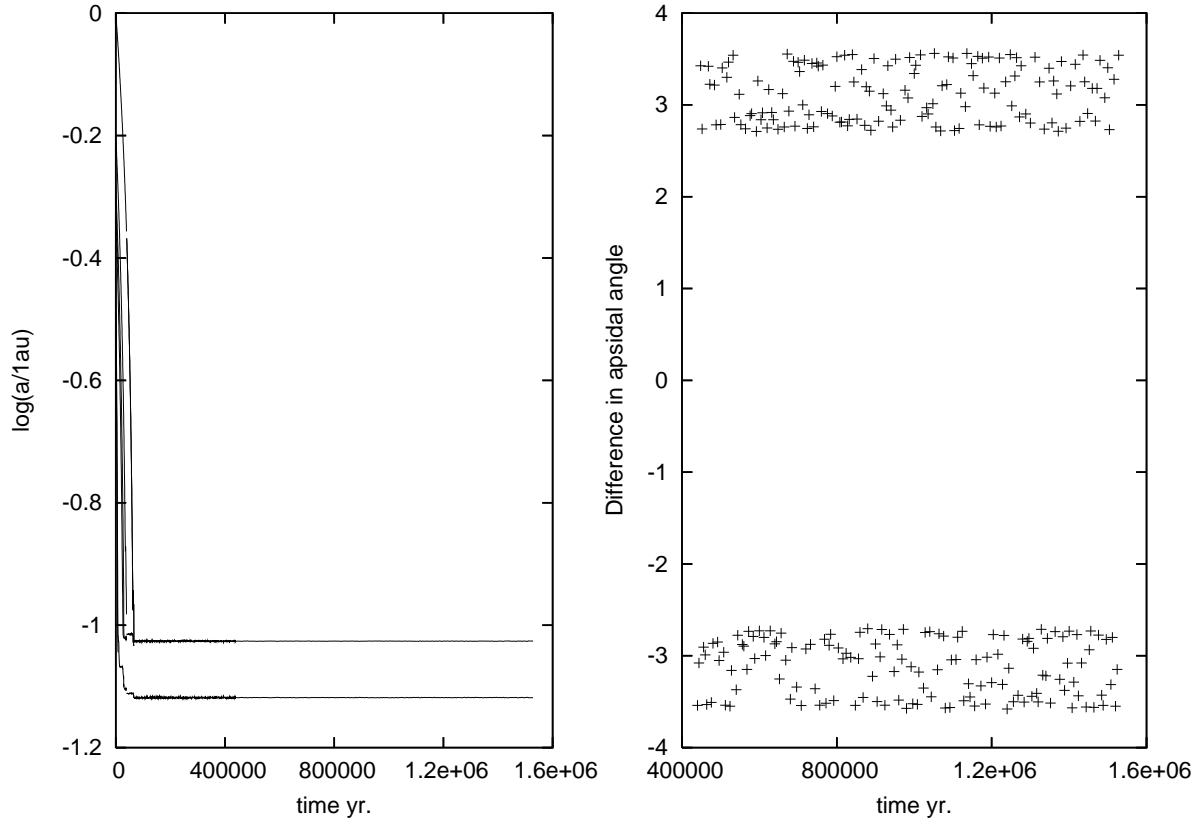


Fig. 5.— The left panel shows, as in figure 4, the evolution of the semi-major axes for run B2 . The right panel shows the evolution of the angular difference of the apsidal lines $\Delta\tilde{\omega}$ (in radians) for the remaining two planets. This oscillates around the anti-aligned position.

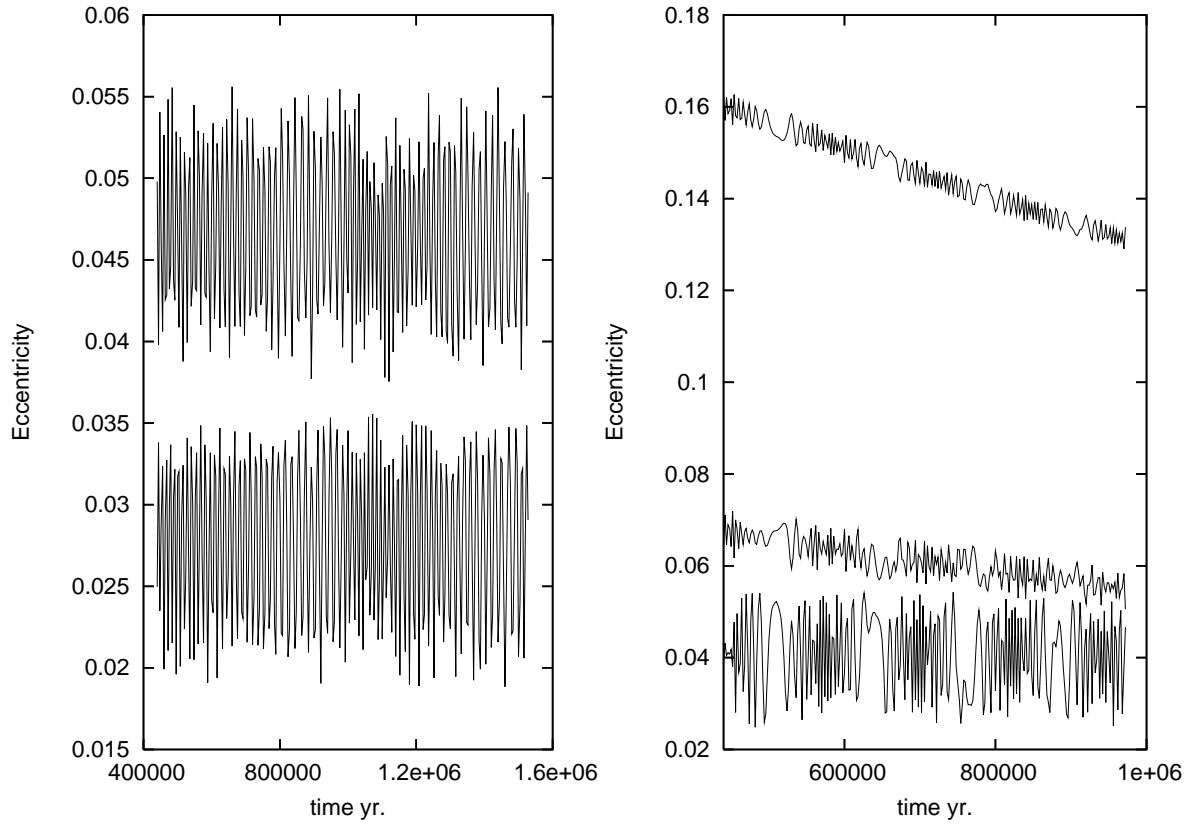


Fig. 6.— The evolution of the eccentricities of the planets in the runs B2 (*left panel*) and A8 (*right panel*). In the former case, the upper curve corresponds to the innermost planet according to semi-major axis. In the latter case, the lowest curve corresponds to the outermost planet and the middle curve to the innermost planet.

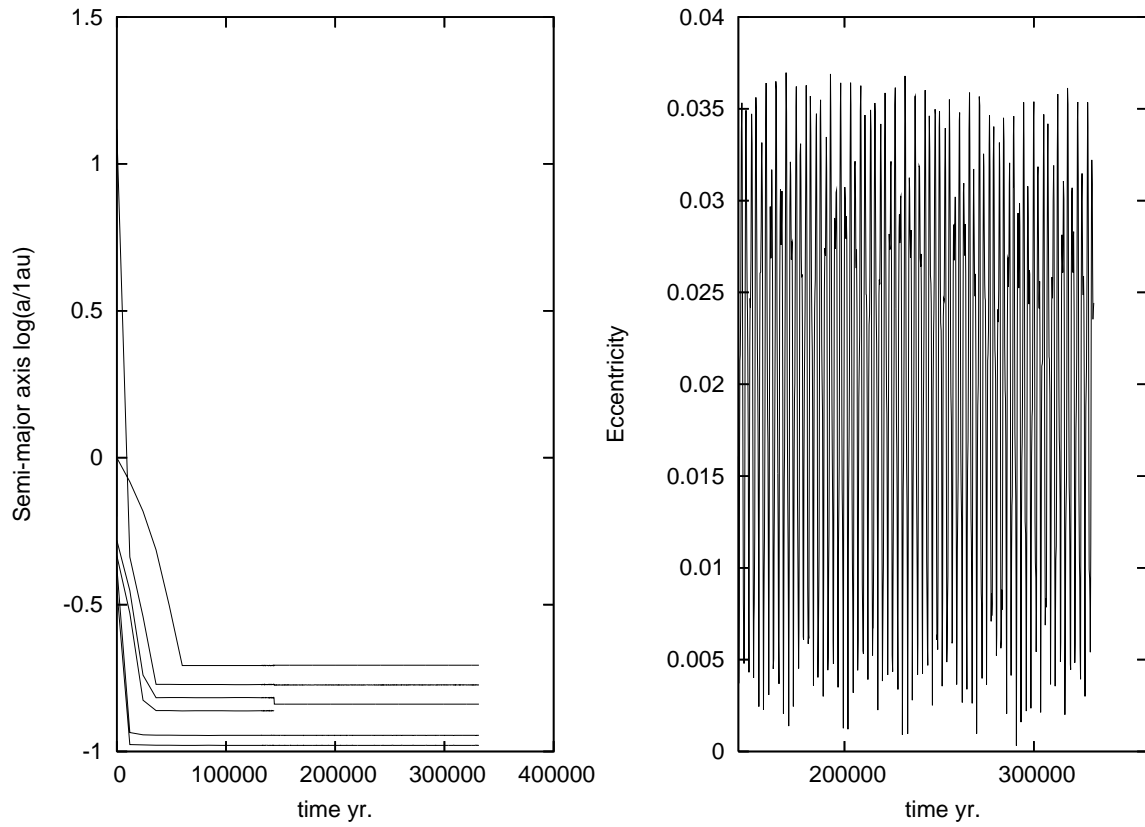


Fig. 7.— The evolution of the semi-major axes (*left panel*) and the later evolution of the eccentricity of the outermost planet (*right panel*) for run C3. In this case, the disk was removed at time 1.32×10^5 yr. Shortly after that time, two of the planets merged leaving a system of five planets.